Claudette G. McKamey
Metals and Ceramics Division
Oak Ridge National Laboratory
P.O. Box 2008, MS-6115
Oak Ridge, TN 37831
Ph. 865-574-6917
Fax 865-574-7659
mckameycg@ornl.gov

Peter F. Tortorelli
Metals and Ceramics Division
Oak Ridge National Laboratory
P.O. Box 2008, MS-6156
Oak Ridge, TN 37831
Ph. 865-574-5119
Fax 865-241-0215
tortorellipf@ornl.gov

Edgar Lara-Curzio
Metals and Ceramics Division
Oak Ridge National Laboratory
P.O. Box 2008, MS-6069
Oak Ridge, TN 37831
Ph. 865-574-1749
Fax 865-574-6098
laracurzioe@ornl.gov

David McCleary
Global Energy Inc.
444 West Sanford Ave.
West Terre Haute, IN 47885
Ph. 812-535-6097
Fax 812-535-6100
dpmccleary@GlobalEnergyInc.com

John Sawyer
Pall Process Equipment Development
3669 State Route 281
Cortland, NY 13045
Ph. 607-753-6041
Fax 607-753-8525
John_Sawyer@Pall.com

Roddie R. Judkins
Fossil Energy Program
Oak Ridge National Laboratory
P.O. Box 2008, MS-6084
Oak Ridge, TN 37831
Ph. 865-574-4572
Fax 865-574-4357
judkinsrr@ornl.gov

Characterization of Field-Exposed Iron Aluminide Hot Gas Filters

Keywords: hot gas filters, iron aluminides, microstructural analysis, mechanical strength

Introduction

The use of a power turbine fired with coal-derived synthesis gas will require some form of gas cleaning in order to protect turbine and downstream components from degradation by erosion, corrosion, or deposition. Hot-gas filtration is one form of cleaning that offers the ability to remove particles from the gases produced by gasification processes without having to substantially cool and, possibly, reheat them before their introduction into the turbine. This technology depends critically on materials durability and reliability, which have been the subject of study for a number of years (see, for example, Alvin 1997, Nieminen et al. 1996, Oakey et al. 1997, Quick and Weber 1995, Tortorelli, et al. 1999).

Materials used in hot-gas filters are required to withstand prolonged exposure to corrosive, high-temperature gaseous environments, as well as to condensable vapors and solid species, some of

which may have the potential for localized interaction with the filter material after extended times. The gas streams may be purely oxidizing (such as those produced by pressurized fluidized bed combustors, PFBCs) or relatively reducing, in which the sulfur species are principally in the form of H_2S, as in the case of the product gas from integrated gasification combined cycle (IGCC) processes or from carbonizers. Degradation of metallic filter elements has been observed under oxidizing, sulfidizing, and/or carburizing conditions and acts as a driving force for the development of ceramic hot-gas filters, particularly for the higher temperatures associated with advanced gasification and combustion designs. However, iron aluminides can also be considered for such applications because they offer reliability advantages over ceramic filters and typically have good to exceptional high-temperature corrosion resistance in a variety of sulfur-bearing environments relevant to coal-derived energy production systems (DeVan 1989, McKamey et al. 1991, DeVan and Tortorelli 1993, Tortorelli and DeVan 1996, Gesmundo et al. 1994, Natesan and Tortorelli 1997, Blough and Seitz 1997, Saunders et al. 1997a, Bakker 1998).

Metallurgical and mechanical evaluations of porous Fe_3Al-based alloys exposed in test beds that simulate environments associated with IGCCs and PFBCs have been conducted (Tortorelli et al. 1998, Tortorelli et al. 1999). Results for as-fabricated porous iron-aluminide filter materials showed good high-temperature corrosion resistance in air, air + SO_2, and H_2S-containing environments. The corrosion resistance was further improved by a preoxidation treatment. The hoop strength of the filters was not significantly affected by the preoxidation treatment or by 100-h exposures in air or air plus SO_2 at 800 and 900°C. The purpose of the current study was to extend such evaluations to iron-aluminide filters that have been exposed in an actual gasification plant. As described below, iron-aluminide filters showed good performance under plant conditions when preoxidation was effective in establishing a thin, protective surface alumina.

Experimental Procedures

Sintered iron aluminide filter elements have been used for hot-gas cleaning at Global Energy Inc.'s Wabash River (Indiana) gasification plant. These cylindrical (~58 mm outer diameter, 2 mm wall thickness) elements were fabricated by Pall Corporation (Cortland, NY) from water-atomized alloy powder produced by Ametek Specialty Metals Division (Eighty-Four, PA). The composition of the powder was nominally Fe-28 at. % Al-2% Cr-0.1% Zr (FAS-Zr). Several pieces of FAS-Zr elements were supplied by Global Energy, Inc. to Oak Ridge National Laboratory after use in the Wabash River Plant's clean-up system. In other cases, o-ring specimens (width of approximately 12.7 mm) were cut from as-fabricated Pall elements, inserted into the filter system at Wabash River for various lengths of operating time, and then returned to ORNL for evaluation. (The general exposure conditions are listed in Table I.) The elements from which the specimens were cut were usually fabricated of FAS-Zr, but in a few cases, o-rings of an FAL alloy composition (Fe-28 at.% Al-5% Cr-0.1% Zr) were exposed. During these exposures, the filter materials were exposed to gas produced by combustion of either coal or petroleum coke at temperatures estimated to be in the range of 450-500°C (see Table I). Note that, in the case of the o-rings, specimens were either placed directly in the filter vessel (dirty-gas side) or in the plenum that routes the filtered gas from the element bundles (clean-gas side).

Evaluation of filter materials included mechanical testing of o-rings by internal pressurization to determine tangential (hoop) stress-strain behavior. The o-rings tested in this manner were from the specimens exposed as such (see above) or were cut from the pieces of actual filter elements received from the Wabash River plant. The internal pressurization tests were conducted in ambient air either by subjecting an elastomeric insert (for as-fabricated filter samples) to axial compression at a constant displacement rate of 2 mm/min or by use of a positive radial-displacement wedge mechanism (for the field-exposed filter samples) (Lara-Curzio 1999). After mechanical testing, the fracture surfaces were examined using scanning electron microscopy (SEM) and pieces were cut from the o-rings for microstructural analysis using optical and SEM, energy dispersive x-ray spectroscopy (EDS), electron microprobe, and Auger electron spectroscopy.

Results

As-fabricated Filter Materials

The as-fabricated filter materials were examined by quantitative image analysis of polished sections. It was determined that they were 40-50% porous with sintered ligaments that ranged between 1 and 30 µm in thickness with a mean value of approximately 9 µm. There were numerous oxide particles on pore surfaces (Fig. 1) and at the boundaries of agglomerated powder particles (Tortorelli et al. 1998). Qualitative analysis by EDS showed that these particles were most likely alumina and zirconia. These oxides form during the water atomization process and most likely coarsened during subsequent processing. After preoxidation at 800-1000°C, the original oxide particles were still clearly evident and a thin protective alumina scale had formed on the metal surfaces. (Pall typically preoxidizes the iron-aluminide filter elements.) Depth profiling by Auger electron spectroscopy showed that the alumina scale formed by preoxidation at 800°C averaged approximately 2 µm in thickness, but could vary between 0.5 and 3 µm. Filters with oxide layers in this thickness range were gray in color. A filter element with various shades of blue also was used to provide o-ring specimens for exposure at the Wabash River Plant. This coloration would indicate a thinner alumina film was formed during preoxidation and, indeed, Auger analysis determined that the oxide coating on the pore surfaces of the blue filter was approximately 0.2 µm. An as-fabricated filter without preoxidation was similarly analyzed and was found to have an alumina layer that was no more than several hundredths of a micron thick.

Determination of the room-temperature tangential stress-tangential strain curves using the elastomeric-insert-internal pressurization approach showed that, when allowance is made for the reduced load-bearing area, the measured strengths of the porous iron aluminides appear to be consistent with those for similar dense alloys (McKamey et al. 1991). The average fracture strength for o-rings cut from two as-fabricated filter elements (IA-187, IA-188, three specimens each) was approximately 2 kN (Table I). Microscopy of the ruptured o-rings showed that failure was transgranular through the fully sintered ligaments and the fracture surfaces were free of oxide particles (Fig. 1). As such, the fracture surfaces were typical of the ductile failures observed for fully dense iron aluminide (McKamey et al. 1991). Preoxidation at 800°C for 7 h had no influence on the hoop strength of the FAS-Zr filter material (Tortorelli et al. 1998).

Specimens from Exposed Filter Elements

Two different samples of the DC-20 filter, exposed for 574 h in the filter vessel at the Wabash River plant, were examined (Table I). The porosity in this filter was non-uniform, with the sample in Fig. 2a showing normal porosity, while the sample in Fig. 2b had less porosity over the inner half of the filter. A light deposit containing S, As, Ge, Si, Cu, Sb, C, Zn, Ca, K, P was observed on the outer surface (that is, the gas inlet side of the filter wall) of both samples. Very little deposit was present on the inner (gas outlet) surface.

The DC-36 filter saw the same exposure conditions as the DC-20 filter, but for a longer time (1565 h). The porosity in this filter was non-uniform, with the inner one-third of the filter having much less porosity than normal (like that shown for DC-20 in Fig. 2b). The outer surface of the filter (at the top in Fig. 2b) contained a light-to-medium deposit consisting of As, Ge, S, Si, and O, while the inner surface had a very light deposit of mostly S and C. Pore surfaces in the interior of the filter were covered with an Al-O product approximately 2 µm thick. Corrosion due to the exposure was not substantial.

Filter element DC-88 was exposed in the vessel at Wabash River for 2185 h. As shown in Fig. 3, microstructural examination indicated that many of the pores in approximately the outer 750 µm of the filter (top in Fig. 3), as well as approximately 300 µm from the inner surface, were almost completely filled. In addition, layers of corrosion products approximately 100 and 50 µm thick were observed on the outer and inner surfaces, respectively. These layers appeared to be growing outward from the filter, since the wall thickness after exposure was about 200 µm greater than before exposure. The fracture strength of this filter element, along with that of DC-36 above, was less than that of the DC-20 and as-fabricated filters (see Table I).

The microstructure and composition of the DC-88 filter element after exposure was characterized using an electron microprobe. Figure 4 shows that the occluded filter region near the outer surface was composed of basically two phases: an Al/Cr-based oxide (see Figs. 4c,f) and an Fe-based sulfide (see Figs. 4b,e). The layer that formed outward from the surface was Fe-S. No areas of Fe_3Al were detected in this 750-µm region near the outer surface, indicating that the entire original Fe-Al-Cr matrix in this area had been consumed by corrosion. The Cr in the original filter material appears to have been incorporated predominantly into the oxide phase (see Fig. 4d). Microprobe analysis showed that the Fe-S layer on the surface also contained many other elements and particles filtered from the gas stream, including oxides of Al and Si, as well as Ni, Zn, Ca, K, Ge, As, and Sb. The occluded region of the inner surface (that is, the outlet side of the filter wall) was also composed of Fe-S and an Al/Cr-based oxide, with a surface layer of Fe-S. The layer also contained a significant amount of As and some Ni, but few, if any, of the other elements that were observed on the outer surface. In the transition regions of the filter, between the completely occluded regions and the porous original matrix still present toward the center of the filter, some of the Fe-Al-Cr matrix phase was detected along with the Fe-S and oxide phases. Figure 5 shows a micrograph and an x-ray scan taken across such a region. The x-ray data revealed the light and medium contrast phases to be Fe-Al-Cr and Fe-S, respectively. The composition of the Fe-Al-Cr phase shown in the x-ray scan is approximately the same as the original filter material, (i.e. Fe-28Al-2Cr), while the composition of the Fe-S phase indicates that it is most likely FeS. A spike in the Al and O levels and

4

a decrease in the Fe level at the interface between these two phases indicate that an oxide layer is still present on the surface of the Fe-Al-Cr particle; presumably it is the Al_2O_3 layer produced by preoxidation. The dark phase is a complex oxide containing Fe, Al, S, and Cr. The layered structure of that phase shown in Fig. 5a and the composition shown in Fig. 5b suggest that it may be an intermediate phase between the Fe-Al-Cr matrix and the FeS/oxide structure present nearer the outer and inner surfaces of the filter.

Specimens Exposed as O-rings

As described in the Experimental Procedures section, o-ring specimens were cut from as-fabricated filter elements and then exposed on the clean- or dirty-gas side of the Wabash River Plant's filtration system. Three o-rings were exposed on the clean-gas side of the filter system without preoxidation: IA-188 for 1628 h, IA-187 for 2237 h and another o-ring of IA-187 for 3865 h. Figure 6 compares the microstructures of these three filter o-rings after exposure. All three o-rings appeared to be blocked with reaction products, with only a small percentage of the pores open toward the outer and inner surfaces of the filter exposed for 1628 h. Higher magnification of the center areas of these filters shows the presence of three main phases (the three levels of contrast in Fig. 7), with the lighter contrast phase (the Fe-Al-Cr matrix) gradually disappearing with time. Analysis of these three phases using EDS showed that, with continued exposure, the Fe-Al-Cr matrix was gradually being converted into oxide and Fe-S products (the dark and medium contrast phases, respectively, in Fig. 7). Higher magnification SEM (Fig. 8) and EDS showed that heavy elements in the coal gas (e.g., As, Ge, Sb) tend to become trapped in the Fe-S phase. For example, the very bright spots in Fig. 8 are particles of As in the Fe-S phase. The results of internal pressurization tests of o-rings from the IA-187 filter exposed for 2237 h showed that the strength was reduced by approximately half in comparison to the as-fabricated filters (Table I).

O-rings from filter elements that had been preoxidized for 7 h at 800°C were exposed on the clean-gas side of the filter system (Table I): DC-207 for 1988 h, IA-191 for 2237 h, and DC-205 for 4335 h. The o-rings exposed for 2237 and 4335 h were in very good condition, with no surface deposits, no reduction in strength, and only minor Fe-S formation throughout the filter. Their microstructures were similar to that observed for the typical unexposed filter (as in Fig. 2a). However, gas flow in the DC-207 o-ring, which had been exposed for only 1988 h, was completely blocked by the formation of almost solid bands of corrosion products on the outside and inside surfaces (see Fig. 9), in addition to corrosion products scattered throughout the interior of the filter (Fig. 10). High magnification SEM (Fig. 9b) and EDS (Fig. 9c) indicated again that the Fe-Al matrix was being converted into Fe-S and oxide products. These results and the results of other analyses discussed above suggest that the iron diffuses outward to fill the pores with Fe-S, a conclusion that has also been reached by others (Bakker and Stringer 1997). The corrosion products formed throughout the thickness of the filter and Fig. 10 shows the Fe-S growing inside the pores in the center of the DC-207 filter.

As part of the study of preoxidation conditions, two o-rings (from filter IA-141) that were preoxidized at 1000°C were exposed for 2237 and 3865 h on the clean-gas side of the plant's filtration system. The microstructures of the o-rings exposed for 2237 and 3865 h were similar to those shown in Fig. 6a,b. Both o-rings appeared to be blocked to the flow of gas although the one exposed for

2237 h still had a noticeable number of unblocked pores. Each had layers of Fe-S on both surfaces, the thickness of which approached 100 μm. High magnification SEM showed an increase in corrosion products and a decrease in the amount of Fe-Al matrix with increasing exposure time, as was shown for the as-fabricated filters in Fig. 7.

As described above, a filter element with a thinner (blue) preformed oxide layer on pore surfaces was used to provide o-ring specimens for exposure at the Wabash River plant. After plant exposure for 1988 h, the o-rings cut from the blue filter (o-rings DC-208 and -211 in Table I) contained only small amounts of corrosion product regardless of location on the clean- or dirty-gas side and their microstructures were similar to that of the as-fabricated filter shown in Fig. 2a. In contrast, o-rings from the gray preoxidized filters exposed at the same time for the same length of time (o-rings DC-209, -210 in Table I) were almost completely blocked by the formation of Fe-S and oxide products (Fig. 11). The presence of such a large amount of the more brittle corrosion products resulted in significantly reduced fracture strengths for the gray o-ring specimens (0.9-1.5 kN, Table I).

Four FAL (see Experimental Procedures section) o-rings were included in the various exposures at the Wabash River Plant and the results are listed at the end of Table I. All the exposed FAL o-rings, whether exposed for 6212 h on the clean-gas side or for 4335 h on the dirty-gas side, exhibited minimal amounts of corrosion products. As expected, the surface deposits on the o-rings exposed on the dirty-gas side were much thicker than on the o-rings exposed on the clean-gas side, but this thicker surface deposit did not affect the appearance, strength (Table I), or filtering capacity of the FAL o-rings.

Strength Measurements

Examination of the strength data reported in Table I indicates an inverse correlation between the amount of sulfidation observed and the fracture stress of the o-ring during loading by internal pressurization. The hoop-strength data, albeit limited, when combined with the microstructural analyses, qualitatively indicate that the iron-aluminide filters maintain approximately their original strength as long as Fe-S formation has not occluded more than approximately 50% of the pores.

Discussion

Evaluation of specimens from plant exposures is complicated by variations in operating conditions from one run to another. Both coal and petroleum coke (higher sulfur content) were used as fuel during the exposure sequences and the temperature was not necessarily the same in each run (probably ranged between 450 and 550°C). In addition, many of the longer exposure times were actually made up of as many as three different campaigns between which the specimens were exposed to unknown lengths of downtime and any possible corrosion associated with such (Bakker 1998, Bakker and Stringer 1997, Saunders et al. 1997b). Nevertheless, this work has yielded some important information about the nature of corrosion of iron aluminides in an operating gasification plant and the effects of composition and preoxidation.

Iron aluminide alloys rely on a thin alumina scale for protection against corrosive environments at high temperatures. For this application, filter elements are normally preoxidized at temperatures

much higher than the gasification filtration unit to assure that a protective alumina film forms. This scale has been observed on preoxidized elements (see above and Tortorelli et al. 1998). In this work, o-ring specimens cut from filters that were not preoxidized and from an element preoxidized at 1000°C were found to be fairly heavily corroded after as little as 1628 h of exposure (see results for IA-141, -187 and -188 in Table I and Figs. 6-8). In contrast, with one exception (DC-207), the o–rings preoxidized at 800°C were still not filled with corrosion products after 4335 h (see results for IA-191, DC-205, -207 in Table I and Fig. 9). Even in the case of DC-207, corrosion was not as severe as in the absence of preoxidation; its fracture strength (which generally tended to decrease with increasing corrosion – see Table I) was equal to the starting material. These results show the importance of the formation of a continuous alumina layer in assuring corrosion resistance during operation of the gasifier and reinforce the need for appropriate and reproducible preoxidation in this regard. [Presumably, the poorer performance of actual filter elements used in the early phases of this study (e.g., DC-88) may have been due to nonoptimal preoxidation.] Preoxidation at 1000°C was not as effective as that done at 800°C. In another study (Pint 2000), the 1000°C preoxidation treatment was found to result in an alumina layer on the filter that was locally disrupted by large zirconia particles and not uniformly continuous and thin. Because of this (and Al depletion concerns – see below), it would not be expected to be as protective as the one formed by preoxidation at 800°C.

Corrosion failure in these filter materials appeared to be associated with the formation of Fe-S inside the pores of the filter. This may mean that sulfidation is kinetically favored under these exposure conditions. However, as described above, Al-containing oxide products were always observed in conjunction with the sulfides. This observation is consistent with a type of breakaway oxidation (sulfidation) in which aluminum is locally depleted by growth of alumina so that, after some point, if the protective scale is breached, iron sulfides form relatively rapidly. The thinness of the ligaments of the filters (mean diameter of 9 µm) magnifies the importance of aluminum depletion/breakaway as the degradation mode because there is a relatively small volume of this element available to form the protective alumina (Quadakkers and Bongartz 1994). This suggested mechanism can explain the better performance of the blue filter materials vis-à-vis the gray ones; Auger analyses have shown a thinner alumina film on the blue material (see above), thereby indicating a greater starting residual aluminum content in the alloy at the time of exposure. The higher aluminum content will increase the time to sulfidation (breakaway). In the same way, the amount of residual aluminum in the filter material preoxidized at 1000°C could be less than what is found in the specimens preoxidized at 800°C and may explain the greater corrosion susceptibility of the former.

The comparison of results from the specimens placed on the dirty- and clean-gas sides, respectively, of the filtration system at the Wabash River gasification plant provides important supporting information regarding the corrosion failure mechanism. As expected, deposits were heavier for those specimens exposed on the dirty-gas side (Table I). However, the extent of corrosion (formation of Fe-S, see above) did not depend on specimen placement. This observation is consistent with the sulfidation degradation mode described above and indicates that the corrosion mechanism is associated with gaseous sulfur and oxygen species rather than the char per se.

As described in the Results section, the preoxidized FAL (Fe-28% Al-5% Cr-0.1%Zr) o-rings were not substantially degraded after exposure for up to 6212 h on the clean-gas side and up to 4335 h on the dirty-gas side of the filtration system – only a relatively small amount of Fe-S was observed. In contrast, after approximately 2000 h, Fe-S was already starting to form in preoxidized filter o-rings made from FAS-Zr powder. Higher chromium concentrations in Fe_3Al-based alloys degrade sulfidation resistance at higher temperatures (DeVan 1989, DeVan and Tortorelli 1993), but may play a beneficial role in this lower temperature gasification plant environment by promoting alumina formation in cases where the oxidized layer is disrupted and/or by improving corrosion resistance at ambient temperatures during downtime (Buchanan et al. 1996). Effects of downtime corrosion can significantly negatively affect subsequent elevated temperature sulfidation (Bakker and Stringer 1997, Saunders et al. 1997b) and may have played a role in the present case for those specimens that saw more than one run cycle during plant exposure. For these reasons, an alumina-forming FeCrAl type of alloy (~20% Cr-5-10% Al) may offer better overall corrosion resistance at the relatively low operating temperatures of the gasification filter system.

Summary and Conclusions

Because of their good to excellent high-temperature corrosion resistance in sulfur-bearing environments, iron aluminide alloys are being evaluated as a potential material of construction for metallic filters to be used to clean fossil-fuel-derived gases prior to their introduction into gas turbines. Iron-aluminide filter-element or o-ring specimens have been characterized after exposure at the Wabash River Plant for times of approximately 400 to 6200 h. Several variables appear to be important to the length of service of these filters, including the preoxidation conditions during fabrication of the filter, time and temperature of exposure, and composition of the iron aluminide. The general mode of corrosion failure involves the formation of iron sulfide that grows into and occludes the pores, resulting in blockage of the filter and reduction in mechanical strength. This process appears to be accelerated at longer exposure times, possibly due to the depletion of aluminum from the filter alloy matrix and the resulting breakdown of the protective alumina layer and its inability to reform. However, with appropriate preoxidation treatments (those that produce a thin protective surface alumina), iron-aluminide filters can have extended lifetimes in coal-derived synthesis-gas environments.

A comparison of o–rings exposed on the clean- and dirty-gas side of the unit showed similar corrosion rates and indicated that the heavier surface deposits produced during exposure on the dirty-gas side does not affect the corrosion process to a significant degree. The filter material of iron aluminide with a higher chromium content tended to experience less degradation. One of these showed good resistance to 6212 h. The limited hoop-strength data generated to date have shown that iron-aluminide filters maintain their original strength as long as Fe-S formation has not occluded more than approximately 50% of the pores.

Acknowledgements

References

Alvin, M. A., 1997. Performance and Stability of Porous Ceramic Candle Filters During PFBC Operation. *Mater. at High Temp*. 14: 285-94.

Bakker, W. T., 1998. Corrosion of Iron Aluminides in HCl Containing Coal Gasification Environments. *Corrosion/98*, NACE Intern., Houston, TX: paper number 185.

Bakker, W. T., and Stringer, J., 1997. Mixed Oxidant High Temperature Corrosion in Gasifiers and Power Plants. *Mater. High Temp*. 14: 35-42.

Blough, J. L., and Seitz, W. W., 1997. Fireside Corrosion Testing of Candidate Superheater Tube Alloys, Coatings, and Claddings — Phase II. *Proc. of Eleventh Annual Conference on Fossil Energy Materials*, Oak Ridge National Laboratory, Oak Ridge, TN: 357-366.

Buchanan, R. A., Kim, J. G., Ricker, R. E., and Heldt, L. A., 1996. Ambient Temperature Corrosion and Corrosive Sensitive Embrittlement. *Oxidation and Corrosion of Intermetallic Alloys*, Purdue University, West Lafayette, IN: 351-419.

DeVan, J. H. 1989. Oxidation Behavior of Fe_3Al and Derivative Alloys. *Oxidation of High-Temperature Intermetallics*, The Mineral, Materials, and Metals Society, Warrendale, PA: 107-115.

DeVan, J. H., and Tortorelli, P. F., 1993. Oxidation/Sulfidation of Iron-Aluminum Alloys. *Mater. High Temp*. 11: 30-35.

Gesmundo, F., et al., 1994. Corrosion of Fe-Al Intermetallics in Coal Gasification Atmospheres. *Materials for Advanced Power Engineering*, Kluwer Academic Publishers: 1657-67.

Lara-Curzio, E., 1999. Oak Ridge National Laboratory, Oak Ridge, TN, unpublished results.

McKamey, C. G., DeVan, J. H., Tortorelli, P. F., and Sikka, V. K., 1991. A Review of Recent Developments in Iron-Aluminum Alloys. *J. Mater. Res*. 6: 1779-1805.

Natesan, K., and Tortorelli, P. F., 1997. High-Temperature Corrosion and Applications of Nickel and Iron Aluminides in Coal-Conversion Power Systems. *International Symposium on Nickel and Iron Aluminides: Processing, Properties, and Applications*, ASM Intern., Materials Park: 265-280.

Nieminen, M., Kangasmaa, K., Kurkela, E., and Ståhlberg, P., 1996. Durability of Metal Filters in Low Sulphur Gasification Gas Conditions. *High Temperature Gas Cleaning*, Universität Karlsruhe, Karlsruhe, Germany: 120-31.

Oakey, J. E., et al., 1997. Grimethorpe Filter Element Performances -- The Final Analysis. *Mater. High Temp*. 14: 301-11.

Pint, B. A., 2000. Oak Ridge National Laboratory, Oak Ridge, TN, unpublished results.

Quadakkers, W. J., and Bongartz, K., 1994. Oxidation Lifetimes. *Werkst. Korros*. 45: 232-38.

Quick, N. R., and Weber, L. D., 1995. Accelerated-Life Testing of Sintered Filters for High-Temperature Corrosive Environments. *Proc. Second International Conf. on Heat Resistant Materials*, ASM Intern., Materials Park, OH: 663-71.

Saunders, S.R.J., *et al.*, 1997a. Behavior of Fecralloy and Iron Aluminide Alloys in Coal Gasification Atmospheres Containing HCl. *Mater. Sci. Forum* 251-254: 583-89.

Saunders, S.R.J., Gohil, D. D., and Osgerby, S., 1997b. The Combined Effects of Downtime Corrosion and Sulphidation on the Degradation of Commercial Alloys. *Mater. High Temp*. 14: 167-73.

Tortorelli, P. F., and DeVan, J. H., 1996. Oxidation and Other Corrosion Phenomena at Intermediate Temperature. *Oxidation and Corrosion of Intermetallic Alloys*, Purdue University, West Lafayette, IN: 267-331.

Tortorelli, P. F., Lara-Curzio, E., McKamey, C. G., Pint, B. A., Wright, I. G., and Judkins, R. R., 1998. Evaluation of Iron Aluminides for Hot Gas Filter Applications. *Proc. Advanced Coal-Based Power and Environmental Systems*, U. S. Department of Energy: paper PB7.

Tortorelli, P. F., McKamey, C. G., Lara-Curzio, E., and Judkins, R. R., 1999. Iron-Aluminide Filters for Hot-Gas Cleanup. *Proc. International Gas Turbine and Aeroengine Congress & Exhibition*, ASME Intern., New York: paper 99-GT-268.
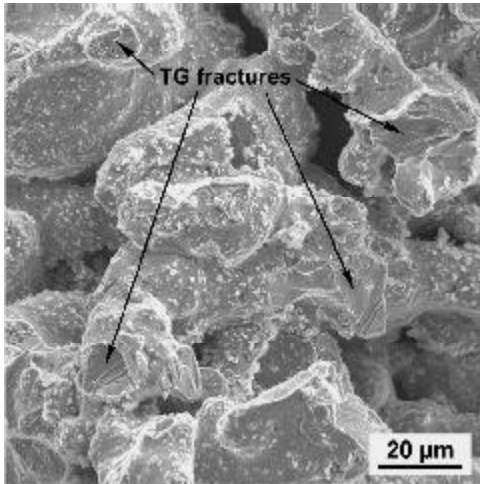
Fig. 1. SEM micrograph of as-fabricated FAS-Zr filter material (IA-187) showing transgranular failure through fully sintered material and oxide particles on powder surfaces.
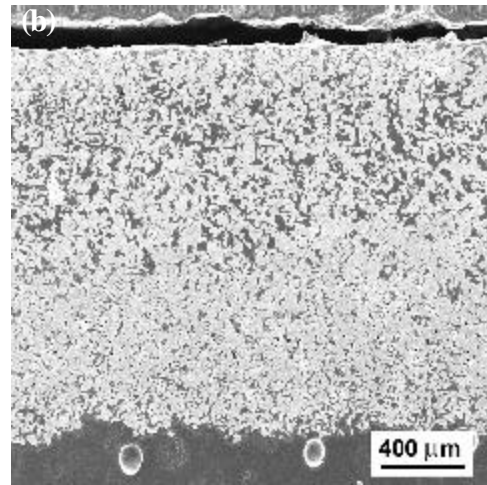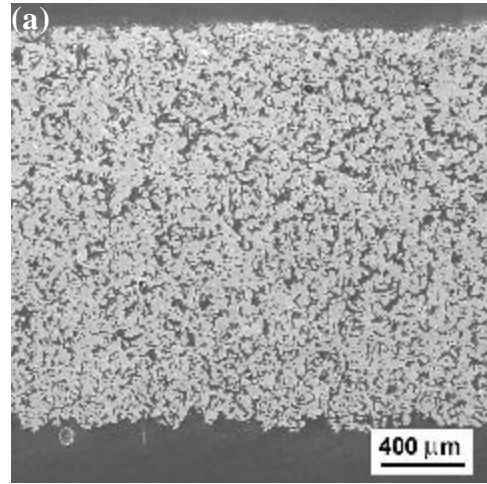
Fig. 2. Microstructures of two different samples of filter DC-20 exposed 1565 h in the Wabash River Energy Ltd plant; (a) showing normal porosity and (b) showing low inner surface porosity. Outer surface (gas inlet side) of filter is at top, inner surface (gas outlet) at bottom.
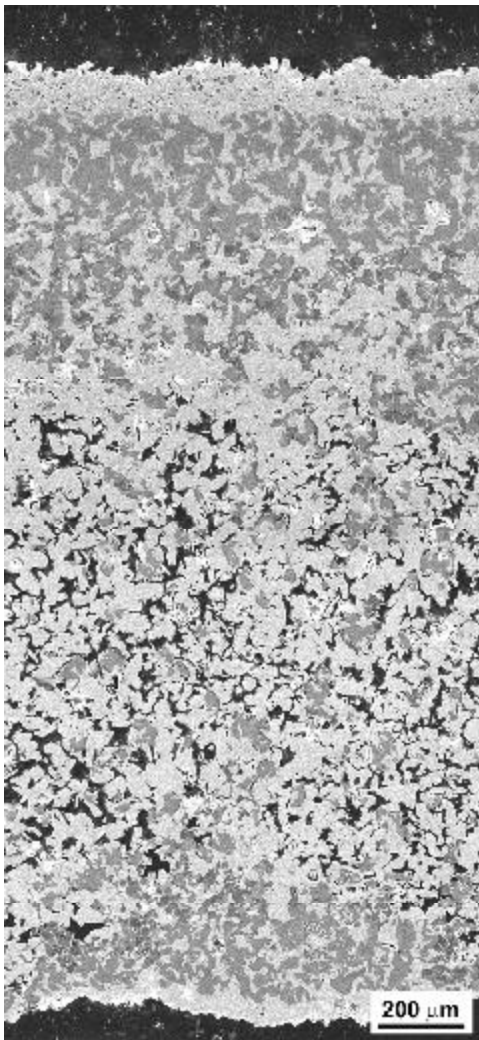

Fig. 3. Microstructure of filter DC-88 exposed for 2185 h in the Wabash River plant.

11
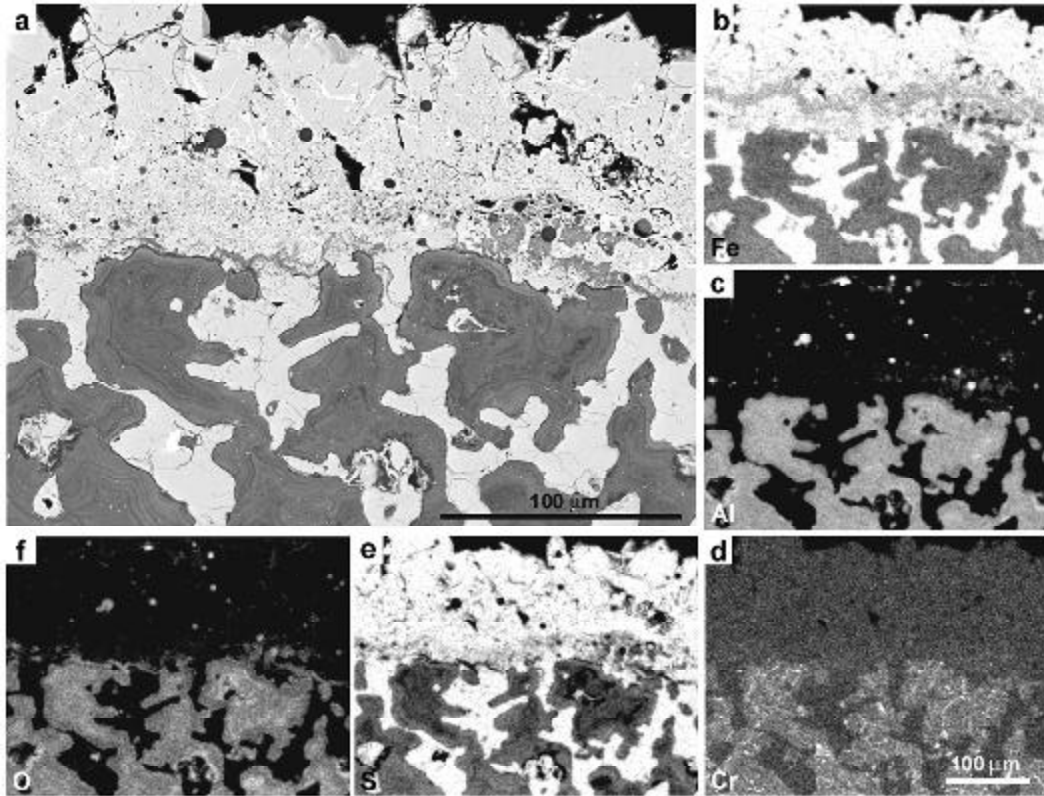
Fig. 4. Backscattered electron image (a) and x-ray mapping for (b) Fe, (c) Al, (d) Cr, (e) S, and (f) O in the outer region of filter DC-88.
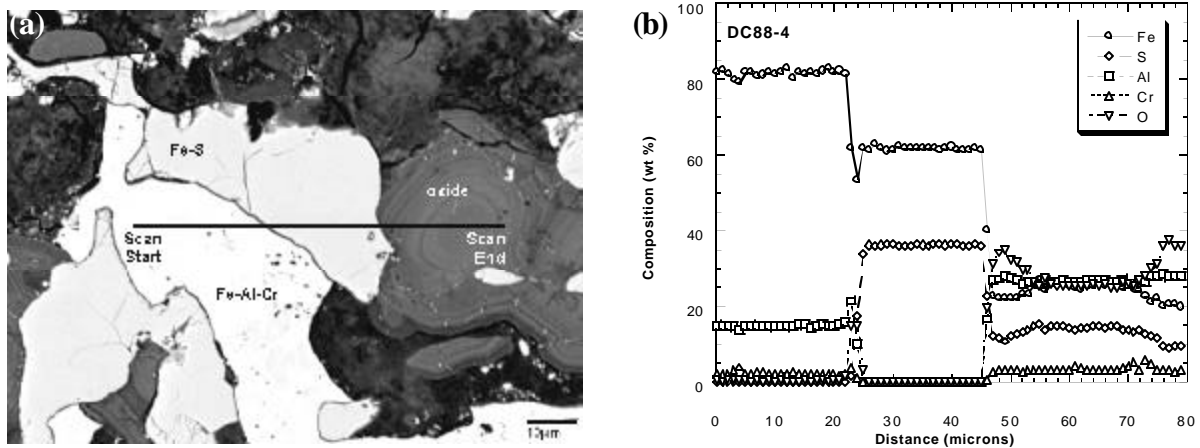
Fig. 5. Backscattered electron micrograph (a) and x-ray scan for Fe, S, Al, Cr, and O (b) across the three different phases observed in filter DC-88 exposed for 2185 h in the Wabash River plant.
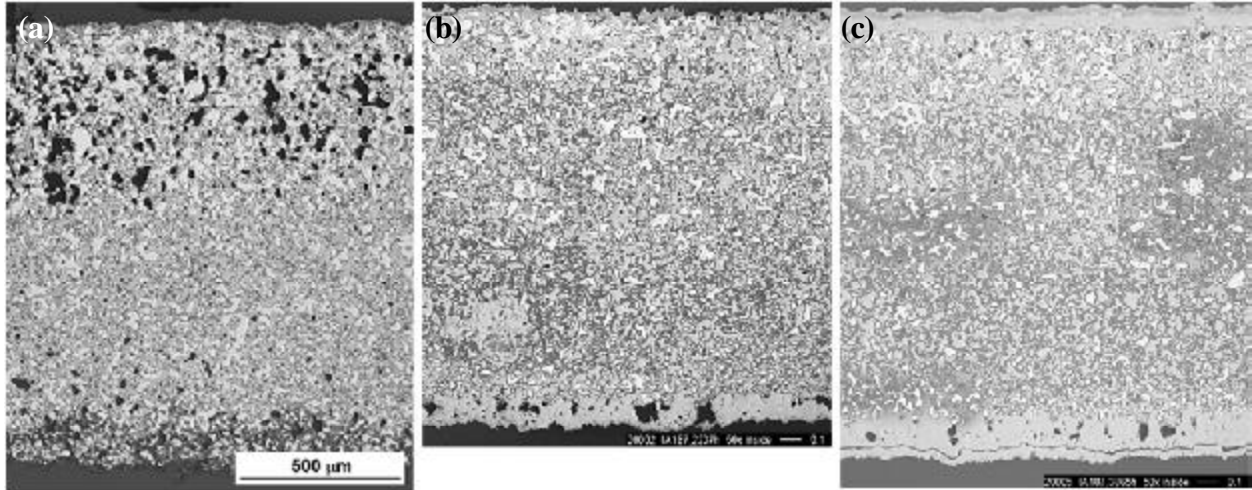
Fig. 6. Optical micrographs showing the microstructures of as-fabricated Fe-Al filters (a) IA-188 after 1628 h, (b) IA-187 after 2237 h, and (c) IA-187 after 3865 h of exposure on the clean-gas side of the Wabash River Plant. Magnifications of (b) and (c) are the same as (a).
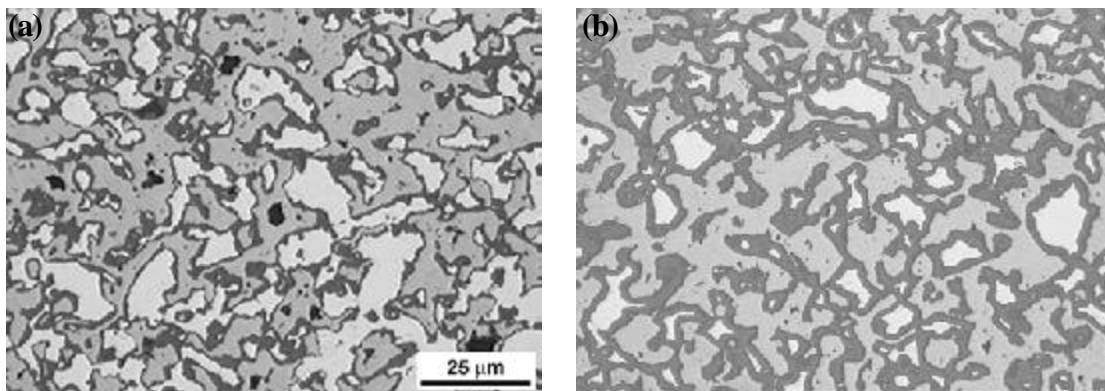

Fig. 7. High magnification optical micrographs showing the microstructures of as-fabricated Fe-Al filters (a) IA-188 after 1628 h and (b) IA-187 after 3865 h of exposure on the clean-gas side of the Wabash River Plant. Magnification of (b) is the same as (a).
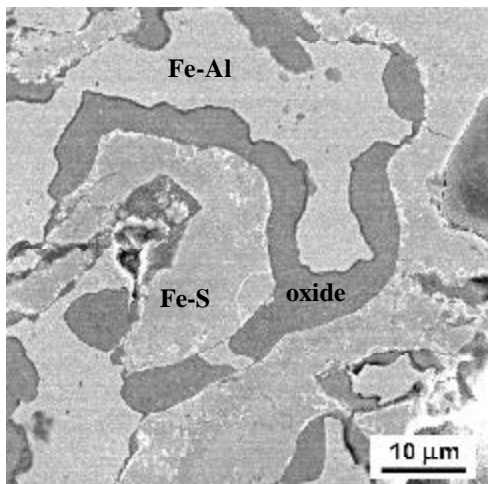

Fig. 8. High magnification optical micrograph showing formation of Fe-S and Al-O phases in as-fabricated Fe-Al filter IA-188 exposed for 1628 h in the Wabash River Plant. White particles in the Fe-S phase are arsenic.
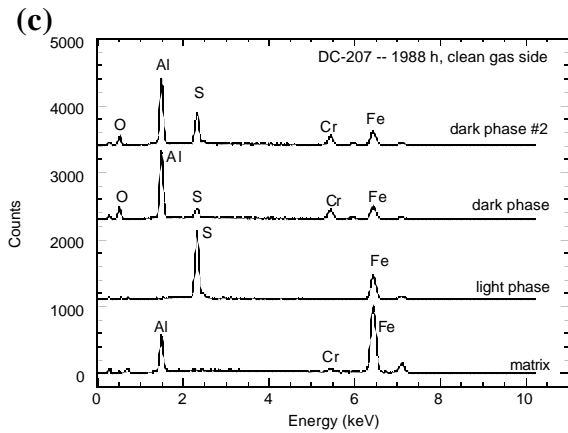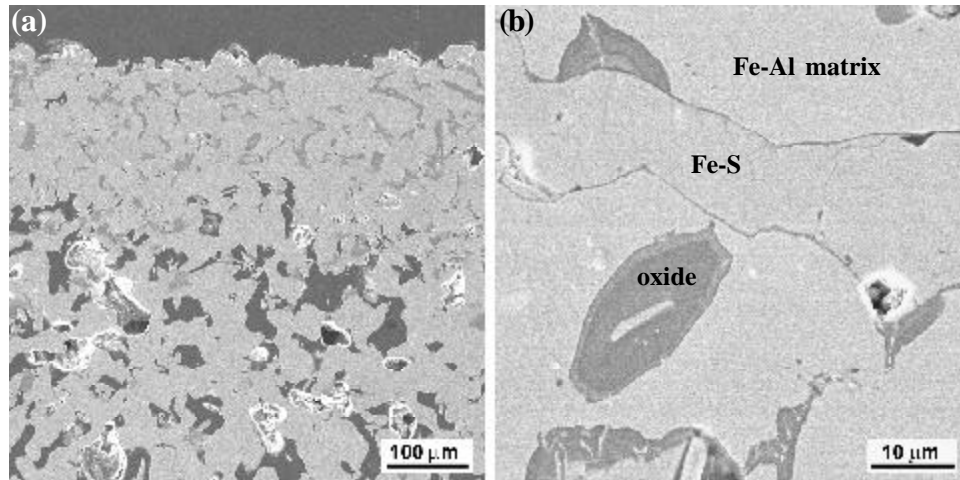
13

Fig. 9. Low- (a) and high-magnification (b) SEM micrographs and (c) EDS spectra for phases present in DC-207 exposed for 1988 h on the clean-gas side.
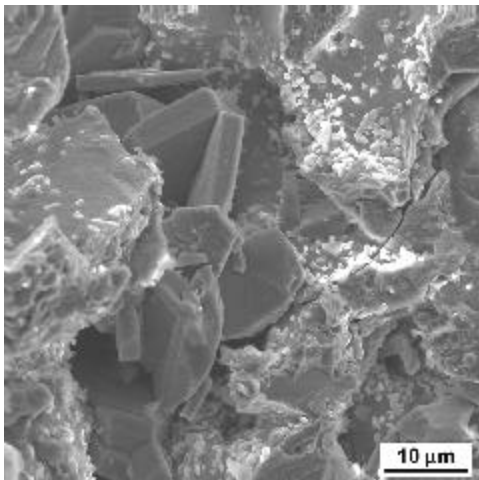

Fig. 10. Iron-sulfur particles forming inside pores in the interior of o-ring DC-207 exposed for 1988 h on the clean-gas side.
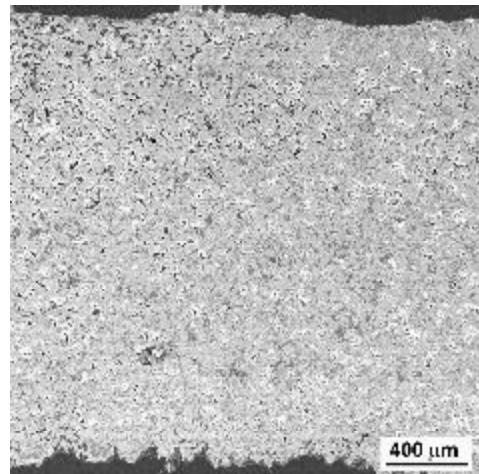

Fig. 11. SEM micrograph showing blocked pores in o-ring DC-209 (from gray filter) after exposure for 1988 h on the clean-gas side of the Wabash River Plant.

14

Table I. Fe-Al Filter Material Exposed at the Wabash River Plant

Filter Design.	Pre-oxidation Temp. (°C)	Exposure time (h)	Exposure details [d]	Results of microstructural analyses	Fracture strength (kN)
IA-187 IA-188 IA-191 IA-141	As fabricated As fabricated 800 1000	None None None None		40-50% porous; oxide particles on pore surfaces; oxide coating on surfaces of 0.5-3 microns thickness; ligaments averaged 6-10 microns	2.0
DC-20[a]	800	574	Vessel	Light surface deposits, some regions of non-uniform porosity	2.0
DC-36[a]	800	1565	Vessel	Non-uniform porosity, pores may be blocked	1.6
DC-88[a]	800	2185	Vessel, 250h petcoke	Fe-S outer layers, blocking gas flow	1.4
IA-188[b]	As fabricated	1628	Clean	Filter blocked by Fe-S throughout inner 2/3 of filter	1.1
IA-187[b]	As fabricated	2237	Clean, 100h petcoke	Filter blocked throughout, thicker deposit on inner surface	
IA-187[b]	As fabricated	3865	Clean, 100h petcoke	Completely full of Fe-S, thick layers on both sides, filter blocked	
DC-207[b]	800	1988	Clean, all petcoke	No surface deposits, large Fe-S layers blocking gas flow, medium interior corrosion	2.2
IA-191[b]	800	2237	Clean, 100h petcoke	No deposits, some Fe-S, filter OK	2.2
DC-205[b]	800	4335	Clean, last ~3000-3500h petcoke	OK, no deposits, some Fe-S throughout	2.2
IA-141[b]	1000	2237	Clean, 100h petcoke	Lots of Fe-S throughout, scattered open pores, may still be filtering	
IA-141[b]	1000	3865	Clean, 100h petcoke	Completely full of Fe-S, thick layers on both sides	
DC-208[b]	800 (blue)	1988	Clean, all petcoke	Light deposit, light corrosion, pores open	2.3
DC-211[b]	800 (blue)	1988	Dirty, all petcoke	Heavy deposit, light corrosion, pores open	2.2
DC-209[b]	800 (gray)	1988	Clean, all petcoke	Medium deposit, heavy corrosion, pores blocked	0.9
DC-210[b]	800 (gray)	1988	Dirty, all petcoke	Heavy deposit, significant corrosion, filter may be blocked	1.5
DC-192[b]	800 (FAL)[c]	2347	Clean, 1000-1500h petcoke	Light-to-medium surface deposits, light corrosion, pores open	1.5
DC-193[b]	800 (FAL)[c]	6212	Clean, 1000-1500h petcoke	Light-to-medium surface deposits, light corrosion, pores open	2.2
DC-195[b]	800 (FAL)[c]	2347	Dirty, 1000-1500h petcoke	Medium-to-heavy surface deposits, light corrosion, pores open	1.4
DC-206[b]	800 (FAL)[c]	4335	Dirty, last ~3000-3500h petcoke	Heavy deposits, light corrosion, pores open	2.0

[a]Specimen from filter element.
[b]Specimen was o-ring cut from filter element.
[c]FAL composition = Fe-28at.%Al-5at.%Cr.
[d]Clean = clean-gas side; dirty = dirty-gas side.